# Evaluation of eCognition Developer and Orfeo ToolBox Performances for Segmenting Agrophotovoltaic Systems from Sentinel-2 Images

Claudio Ladisa[1], Alessandra Capolupo[1(✉)], Maria Nicolina Ripa[2], and Eufemia Tarantino[1]

[1] Department of Civil, Environmental, Land, Construction and Chemistry (DICATECh), Politecnico Di Bari, via Orabona n. 4, 70125 Bari, Italy
{claudio.ladisa,alessandra.capolupo,eufemia.tarantino}@poliba.it
[2] Department of Agricultural and Forest Sciences (DAFNE), Università Degli Studi Della Tuscia, Via S. Camillo de Lellis Snc, 01100 Viterbo, Italy
nripa@unitus.it

**Abstract.** A deep energy transformation will be tried out across the globe in the next decades in order to detect potential green and renewable sources able to replace fossil fuels. Among the various alternatives, photovoltaic technology, recognized as sustainable, clean, and environmentally friendly essence, is considered one of the most relevant solutions. To date, the Remotely Piloted Aircraft System has been largely used to inspect solar parks albeit the treatment of very high-resolution satellite images through object-based models may be a valid option. In this work, the potentialities of two segmentation approaches (multi-resolution and mean-shift algorithms, implemented in eCognition Developer and Orfeo Toolbox software, respectively) in extracting photovoltaic panels from Sentinel-2 time series were explored and compared. Such techniques were tested in Montalto di Castro in Viterbo (Italy). Multi-resolution algorithm was applied by varying scale and shape parameters between 20 and 100 and 0.1 and 0.5, respectively. Conversely, the mean-shift approach was used by considering the default values of spatial radius and range radius. Their segmentation outcomes were compared on the base of i) minimum Euclidean Distance 2 (ED2), calculated in AssesSeg environment, ii) segmentation polygons statistics and areas value, and, lastly, iii) their performance in terms of processing time, versatility, ability of handling heavy data, and cost. ECognition Developer demonstrated a better performance in segmenting Sentinel 2-images for extracting PV systems in terms of segmentation parameters management and outcomes interpretation ability.

**Keywords:** Object-Based Image Analysis (OBIA) · Segmentation · Agrophotovoltaic panels · Copernicus Program · Medium-resolution satellite images

© The Author(s), under exclusive license to Springer Nature Switzerland AG 2022
O. Gervasi et al. (Eds.): ICCSA 2022 Workshops, LNCS 13379, pp. 466–482, 2022.
https://doi.org/10.1007/978-3-031-10545-6_32

## 1 Introduction

The need to tackle climate change and the imminent depletion of oil, coal, and natural gas reserves is leading the World to rely on renewable sources such as solar, wind, biomass, and geothermal energy [1]. Currently, the actual green energy capacity is expected to grow of about 50% by 2024 [2]. The strong, though now stable, construction and design costs decline, mainly due to the higher energy productivity of PV modules, have promoted PV deployment albeit PV solar installation implies a consistent soil loss [3]. As shown in the statistical report edited by the Gestore Servizi Energetici (GSE) in 2019 [4], 880,090 PV systems, with a total capacity of 20.865 MW, were installed up to December 31, 2019, in Italy. 92% of them were small systems with a power less than or equal to 20 kW. and an average system size of 23.7 kW. Nevertheless, the land is considered a commodity and, thus, specific studies have been carried out to investigate PV impact on land use [5, 6]. For this reason, in recent years, agrovoltaic or agrophotovoltaic systems have been implemented to allow the simultaneous cultivation and production of renewable energy, reducing high land consumption [7]. The choice of the adequate lands where to install PV systems is affected by many factors, such as geographical position, morphological characteristics of the territory and climatic conditions. As a result, their distribution is very heterogeneous among the different regions [4]. An additional key factor to be considered concerns the defects brought out by their permanent exposition to harsh environmental conditions [8]. Therefore, a constant inspection of their health status performed with various methods, such as field-of-view diagnosis, infrared thermal imaging, and electricity-based techniques, is required [1]. All these traditional techniques have proven to be obsolete for monitoring large structures and, therefore, valid alternatives based on digital image analysis have been introduced [9]. Remotely Piloted Aircraft System (RPAS) image-based assessment systems are considered as the optimal solution to meet such a purpose because of its competitive costs and the fastness of monitoring the efficiency of systems made up of many photovoltaic modules [10]. Nevertheless, the development of many large-scale PV systems in recent years has made RPAS an ineffective technique for monitoring them [11, 12]. The recent introduction of free medium and high-resolution satellite images could go beyond those limitations. Among the several techniques developed to process them, the object-based analyses are mainly adapted to extract land use/land cover information [13–16]. Object-Based Image Analysis (OBIA) principle is to group together spectrally and geomorphologically similar pixels to form objects which will be then classify [13, 17, 18]. The step allowing object identification is commonly called “Segmentation”. This step can be performed by applying various software, such eCognition Developer (Trimble, Sunnyvale, California, USA) and Orfeo Toolboxes (OTB). As demonstrated by previous works [19], eCognition Developer is suitable for segmenting satellite images or mosaics at larger scales because of its ability of producing a number of segments closer to the number of objects defined as ground truth data and its processing speed. Nevertheless, it cannot be applied in the projects with limited budgets because of its high license cost. On the other hand, OTB is a free open-source software able to generate satisfying outcomes albeit it needs a high processing time [20]. ECognition Developer and OTB were used for extracting PV systems and roofs from satellite data by Xia et al. [21] and Khan et al. [22], respectively. Both works showed satisfying results without any excessive

computational costs. Nevertheless, Plakman et al. [23] demonstrated an improved of PV systems extraction outcomes using Sentinel-2 (S2) satellite images thanks to the many spectral bands provided by the sensor mounted on it. To the best of authors' knowledge, any researches based on the combination of the two above-mentioned software and S2 images have not been proposed in the literature for extracting PV systems. In this paper, the performance of eCognition Developer environment, a leading commercial software, and the open-source OTB for extracting PV solar panels from S2 time series were evaluated and compared. To achieve such an objective, two different segmentation algorithms (multi-resolution and mean-shift) were tested on the experimental site of Montalto di Castro, located in Viterbo, Italy. Such a site was selected because of the presence of the largest solar parks in Europe up to 2011. Software' outcomes quality as well as its ability and versality were evaluated by computing the modified version of Euclidean Distance (ED2) index, statistical metrics of the generated segmented polygons and processing time.

## 2 Study Area

The pilot site is located in Montalto di Castro, 42 km far from Viterbo city (northern part of Lazio Region, Central Italy) (Fig. 1).

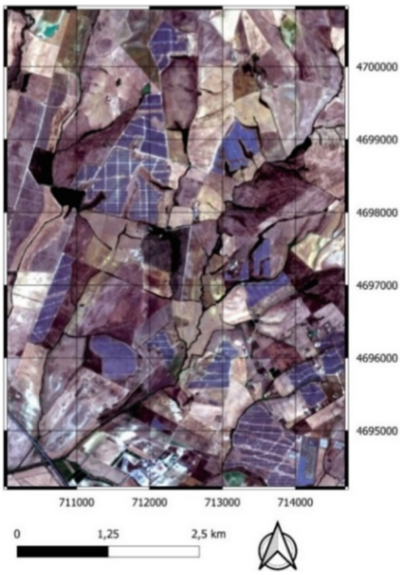


**Fig. 1.** Study site world geodetic system 84 Universal Transverse Mercator (UTM) zone 32N.

Such rectangular area covers a surface of about 6.2 $km^2$, characterized by a predominant flat morphology. It was selected as a test site due to the presence of the largest photovoltaic plant system in Europe up to 2011[24, 25], subsequently blocked-in accordance with the Italian Ministry for Cultural Heritage activities and tourism, worried

about its impacts on cultural heritage landscapes, archaeological and historical areas, located close by [26].

## 3 Datasets

### 3.1 Sentinel-2 Imagery

Ten cloud-free Sentinel-2 (S2) scenes were collected over the study area from the European Space Agency (ESA) Copernicus Scientific Data Hub instrument website [27] (Table 1). Level 2A (L2A) was selected and all data were provided in World Geodetic System 84 (WGS84) Universal Transverse Mercator (UTM) zone 32N. The S2 multispectral (MS) sensor collects up to 10 bands with three different geometric resolutions ranging from 60 up to 10 m. Among them, four bands (Blue (B): 458–523 nm, Green (G): 543–578 nm, Red (R): 650–680 nm and Near Infrared (NIR8): 785–900 nm) have a resolution of 10 m, while six bands (Red Edge 1 (RE1): 694–713 nm, Red Edge 2 (RE2): 731–749 nm, Red Edge 3 (RE3): 769–797 nm, Narrow Near InfraRed (NIR8a): 848–881 nm, Shortwave Infrared-1 (SWIR1): 1565–1655 nm and Shortwave Infrared-2 (SWIR2): 100–2280 nm) have a resolution of 20 m. In this study, both 10 m and 20 m resolution bands were used because of the low reflectance of solar panels in VIS and NIR spectrum [28]. Lastly, S2 images were clipped in Quantum GIS (QGIS) environment (version 3.22) on the selected study area.

**Table 1.** Input Sentinel-2A and Sentinel-2B images.

| Date of acquisition (D/M/Y) | Sensor | Orbit | Level |
|---|---|---|---|
| 24/02/2021 | S2B | R122 | 2A |
| 31/03/2021 | S2A | R122 | 2A |
| 25/04/2021 | S2A | R122 | 2A |
| 28/05/2021 | S2B | R022 | 2A |
| 29/07/2021 | S2A | R122 | 2A |
| 21/08/2021 | S2A | R022 | 2A |
| 30/09/2021 | S2A | R022 | 2A |
| 30/10/2021 | S2A | R022 | 2A |
| 24/11/2021 | S2B | R022 | 2A |
| 31/12/2021 | S2B | R122 | 2A |

## 4 Software

### 4.1 eCongnition Developer 9.5

eCognition is a powerful object-based environment for image analysis [29]. It classifies and analyzes images, vectors, and point clouds using all the semantic information needed

to interpret them correctly. It does not examine single pixels or points, but it investigates the mutual relationships among neighboring pixel of the same layer and across various input data [29]. Thus, similar pixels are generally grouped together in objects[29]. ECognition suite offers three different components that can be used individually or in combination to solve the most challenging image analysis tasks: i) eCognition Developer; ii) eCognition Server and, lastly, iii) eCognition Architect. ECognition Developer is a software created for object-based image analysis. It is widely used in the field of remote sensing because of the simplicity of creating rule sets suitable for performing automatic data analysis. It contains a large collection of algorithms that can be combined to facilitate rapid development of geospatial analysis applications [29]. The eCognition Server software is a processing environment for simultaneous multiple data development and transferability testing, while eCognition Architect enables non-technical professionals to perform OBIA. Users can easily customize the ruleset created a proper rule-based model in eCognition Developer [29].

### 4.2 Orfeo ToolBox

Orfeo ToolBox is an open-source project for satellite data investigation [30]. Based on the backs of the open-source geospatial community, it can process optical, multispectral, hyperspectral and radar resolution imageries up to the terabyte scale. Therefore, it can be applied by a wide variety of applications, including orthorectification, pansharpening, supervised and unsupervised classification, feature extraction. All the implemented algorithms are accessible from Monteverdi, QGIS [30], Python, command line, and C++. Monteverdi is a visualization tool that allows users looking at high-resolution images and accessing all toolbox commands [30]. It is available on Windows, Linux, and Mac OS X.

### 4.3 AssesSeg

AssesSeg is a command line tool based on the computation of the modified version of the Euclidean supervised Distance (ED2) aimed at assessing the segmentation quality by calculating the Potential Segmentation Error (PSE) and the Number-of-Segments Ratio (NSR). These two parameters measure the geometric and the arithmetic discrepancy between the manually digitized ground truth and the corresponding segments, respectively. A high ED2 value indicates a high geometric and/or arithmetic discrepancy, while a low ED2 value implies a good level of segmentation [31]. AssesSeg's goal is to evaluate segmentation quality [31]. It was produced by the cooperation between the University of Almeria (Almeria, Spain) and the Politecnico di Bari (Bari, Italy). AssesSeg outputs allow detecting the best bands combination and showing a clear positive correlation between segmentation accuracy and the amount of available reference data [31].

### 4.4 Quantum GIS (3.22)

QGIS is an open-source Geographic Information System (GIS). The project was born in May 2002, and it was established by SourceForge in June of the same year. Currently, it

runs on the most relevant platforms, such as, for instance, Unix, Windows, and macOS. It is developed using the Qt toolkit [32] and C++ [33]. Its intuitive graphical user interface (GUI) allows users conducting advanced GIS analysis easily [33]. QGIS supports a huge number of raster and vector data formats, and many free plug-ins can be downloaded for any geomatics applications. [33].

## 5 Methodology

The digitalization of PV panels located in the study area allows having the Ground Truth for assessing segmentation quality. Thus, after digitalizing the solar park manually, the operative workflow reported in Fig. 2 was applied. Once S2 images were collected, they were segmented in eCognition Developer and OTB software separately. A multi-parameter approach, based on scale, shape, and compactness parameters, was applied in eCognition platform.

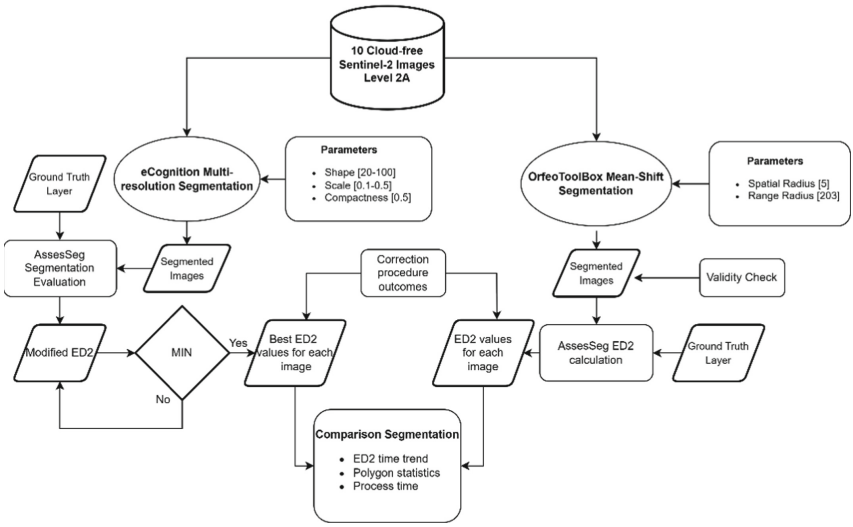


**Fig. 2.** Workflow of the applied methodology.

A mean-shift segmentation algorithm was, instead, used in OTB platform. Contrary to the technique adopted in eCognition, fixed values were picked up in this case. Then, for each segmented image, ED2 was calculated. The smallest ED2 value corresponds to the best segmentation parameter set for each image. ED2 outcomes were compared. Some output segmentations from the two software that showed abnormal ED2 values were subjected to correction procedures, aimed at masking all pixels characterized by an anomalous reflectance value. Lastly, software performances were also investigated in terms of processing time, versatility, and costs.

### 5.1 Multi-resolution Segmentation in eCognition

The Multiple Resolution Image Segmentation (MRS) algorithm, already implemented in the eCognition Developer environment, was applied to gathered S2 images. MRS performance depends on three main parameters: (i) Scale parameter (SP), responsible for defining the maximum admissible heterogeneity. The larger the value, the larger the resulting objects is [29]. SP ranged between 20 and 100 (with an increment step of 1.0); (ii) the weight of color and shape criteria (Shape), which assigns a weight to the shape and spectral color of the objects. When the shape weight is zero, only the value assigned to col-or is considered, while when it is greater than zero, the shape of the objects is taken into account along with the color [29]. It was between 0.1 and 0.5 (with an increment step of 0.1); lastly, (iii) the weight of compactness and smoothness (Compactness) criteria useful for optimizing overall compactness [29]. It was set at 0.5 for all cases. As proposed by Novelli et al. [34], the optimal combination of MRS parameters was selected by applying AssesSeg.

### 5.2 Mean-Shift Segmentation in OTB

The Mean-Shift algorithm is an iterative process consisting on the shift of each single data point toward the average of the data points in its proximity [35]. Two parameters control the segmentation process: i) the spatial radius, responsible for the pixels number to be grouped into the segmented images, and ii) range radius, defining the objects of interest size. [36]. For this reason, several tests are required to select the optimal parameters. The range radius was set equal to the average number of pixels within the Ground Truth segments. Instead, for the spatial radius, the default value was used in OTB.

### 5.3 Comparative Assessment

Three methods were used to compare the segmentations: i) evaluation of the time trend of ED2 index; ii) estimation of the descriptive statistics of polygon geometries and Ground Truth; iii) assessment of the processing times to perform the segmentation procedures. The total number of polygons provides information on the detail level that can be captured as well as the time needed to run the segmentation procedure and basic analytic analysis, such as raster conversion into vector and zonal statistics computation [19]. The area was calculated for each polygon using the ‘field calculator’ tool implemented in QGIS environment. A set of descriptive statistics (minimum, maximum, range, sum, mean, median and standard deviation) was also evaluated through the “basic field statistics” tool. The metrics extracted from Ground Truth and polygons were explored. Images reporting an anomalous ED2 values were subsequently corrected by masking all pixels with inconsistent reflectance values. Then, the whole procedure was applied again on the corrected maps.

# 6 Results

## 6.1 Multi-resolution Segmentation Outputs

Figure 3 reports the trends of the modified ED2 index for all the segmented images produced by applying eCognition Developer. Most of the images reach the lowest ED2 value setting the shape equal to 0.5 and the scale ranges between 36 and 55.

The best ED2 value (0.454) was shown from the image acquired in August using 53 and 0.3 for the scale and the shape, respectively. On the other hand, instead, the images belonging to October and November reported an anomalous trend and November showed the highest value of ED2 and scale. Scale and shape values useful to obtain the corresponding minimum ED2 value for each image is reported in Table 2.

## 6.2 Mean-Shift Segmentation Products

Table 3 describes the ED2 values computed on the images segmented using the Mean-Shift Segmentation algorithm. Even in this case, the lowest ED2 value was generated in August while November reported an anomalous trend. In this case, the ED2 value registered for October is in line with that one obtained in the other months.

## 6.3 ED2 Trend Comparison Outcomes

Figure 4 describes the trend of the minimum value of ED2 obtained by processing the images in eCognition Developer and OTB, respectively. A quite similar trend is detected using both software from February till September. Such a Figure enhances the anomalies already noted in November and October outcomes generated using eCognition Developer. Also OTB shows an anomaly in November albeit it is less marked. On the contrary, any anomalies are not detected in OTB for October.

## 6.4 Polygons Statistics Results

Tables 4 report the total amount of obtained polygons generated using eCognition Developer and OTB, respectively. Furthermore, the number of polygons intersected with Ground Truth is shown too. ECognition Developer produced more polygons than OTB except in November. Polygons intersecting Ground Truth are greater in eCognition Developer than in OTB.

Figure 5 shows the metrics calculated on the polygons intersected with the Ground Truth samples. In particular, in Fig. 5a, it can be seen that the areas of the polygons intersected with Ground Truth, produced by OTB, have a higher average value than those obtained from the Ground Truth polygons for all months under analysis, while eCognition Developer produced results with a more fluctuating trend always below the average value of Ground Truth, except in September. In Fig. 5f, the coefficient of variation (CV) values show more heterogeneity in the polygons generated by eCongnition Developer. The values of standard deviation, median, CV and minimum show more small segments for eCognition Developer in November. Table 5 describes the processing time needed in eCognition Developer and OTB, respectively. eCognition Developer time involves

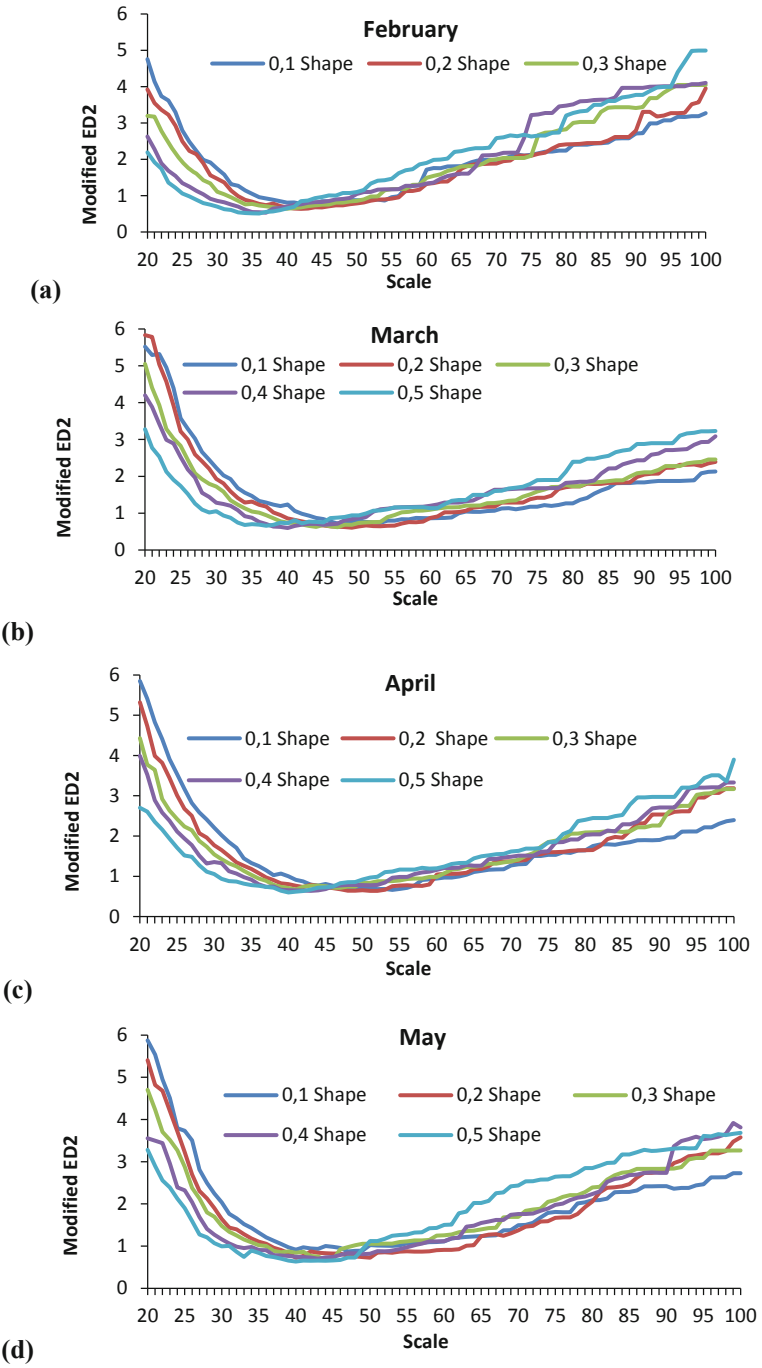


**Fig. 3.** ED2 value trend computed on the images collected in: (a) February; (b) March; (c) April; (d) May; (e) July; (f) August; (g) September; (h) October; (i) November; (j) December.

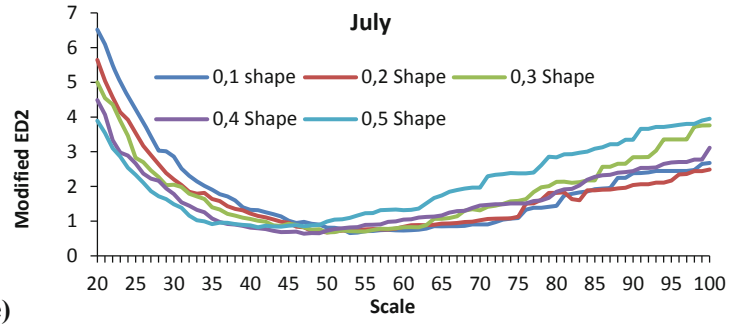


(e)

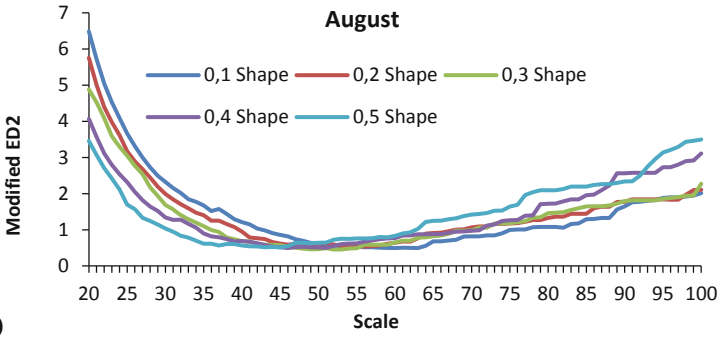


(f)

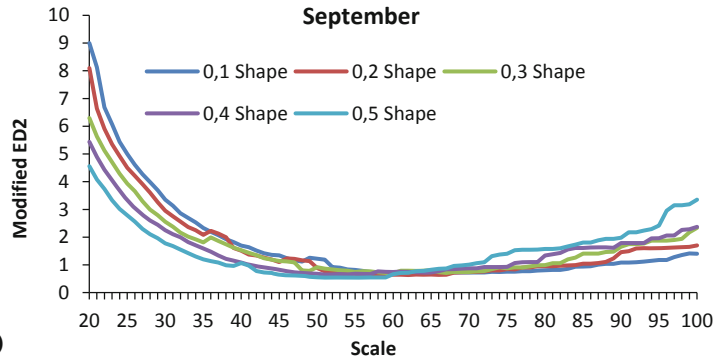


(g)

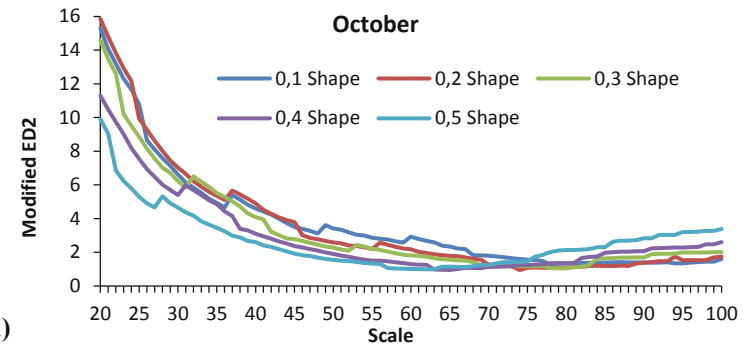


(h)

**Fig. 3.** continued

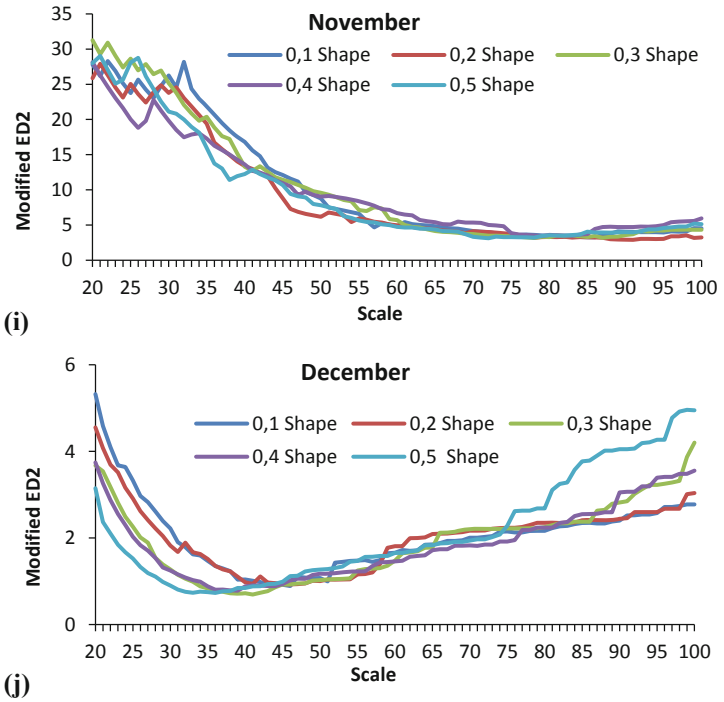


**Fig. 3.** continued

**Table 2.** Best Shape and Scale values obtained using eCognition Developer.

| Month | Minimum ED2 | Scale | Shape |
|---|---|---|---|
| February | 0.507 | 36 | 0.5 |
| March | 0.598 | 40 | 0.4 |
| April | 0.599 | 40 | 0.5 |
| May | 0.632 | 40 | 0.5 |
| July | 0.641 | 47 | 0.4 |
| August | 0.454 | 53 | 0.3 |
| September | 0.537 | 55 | 0.5 |
| October | 0.942 | 74 | 0.2 |
| November | 2.895 | 91 | 0.2 |
| December | 0.695 | 41 | 0.3 |

the whole time required to carry out the complete segmentation procedure including the variation of the parameter, as specified in the previous paragraph. Conversely, OTB time is referred just to a single segmentation since the default value are used. In both

**Table 3.** Best shape and scale values obtained using OTB.

| Month | Minimum ED2 | Spatial radius | Range radius |
|---|---|---|---|
| February | 0.651 | 5 | 203 |
| March | 0.573 | 5 | 203 |
| April | 0.627 | 5 | 203 |
| May | 0.660 | 5 | 203 |
| July | 0.712 | 5 | 203 |
| August | 0.559 | 5 | 203 |
| September | 0.707 | 5 | 203 |
| October | 0.716 | 5 | 203 |
| November | 1.023 | 5 | 203 |
| December | 0.743 | 5 | 203 |

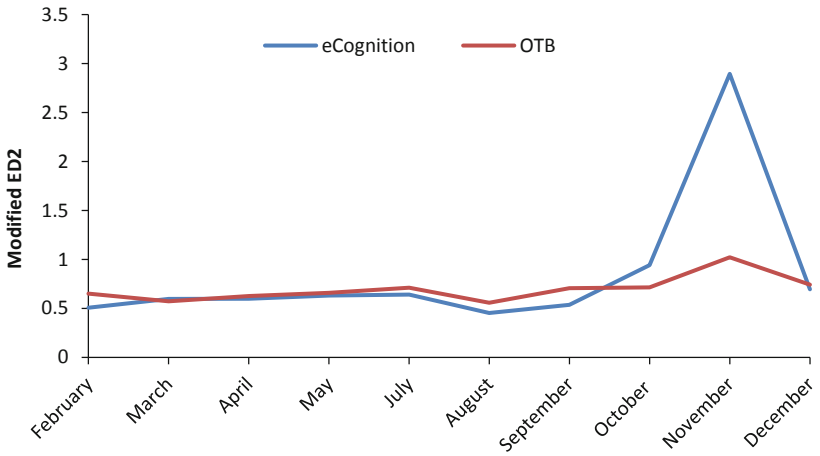


**Fig. 4.** Comparison of ED2 trends extracted using eCognition Developer (in blue) and OTB (in orange). (Color figure online)

**Table 4.** Statistics of eCognition Developer and OTB polygons. GT: Ground Truth.

| | | GT | Feb. | Mar. | Apr. | May | Jul. | Aug. | Sept. | Oct. | Nov. | Dec. |
|---|---|---|---|---|---|---|---|---|---|---|---|---|
| eCognition | Pol | 152 | 4428 | 5055 | 4271 | 4210 | 4242 | 3917 | 2943 | 2623 | 1979 | 4719 |
| | Inters. pol. & GT | \ | 409 | 477 | 417 | 416 | 381 | 369 | 333 | 425 | 498 | 474 |
| OTB | Pol | 152 | 2586 | 2332 | 2640 | 2597 | 2556 | 2577 | 2501 | 2539 | 2586 | 2545 |
| | Inters. pol. & GT | \ | 326 | 319 | 332 | 320 | 329 | 331 | 306 | 314 | 322 | 317 |

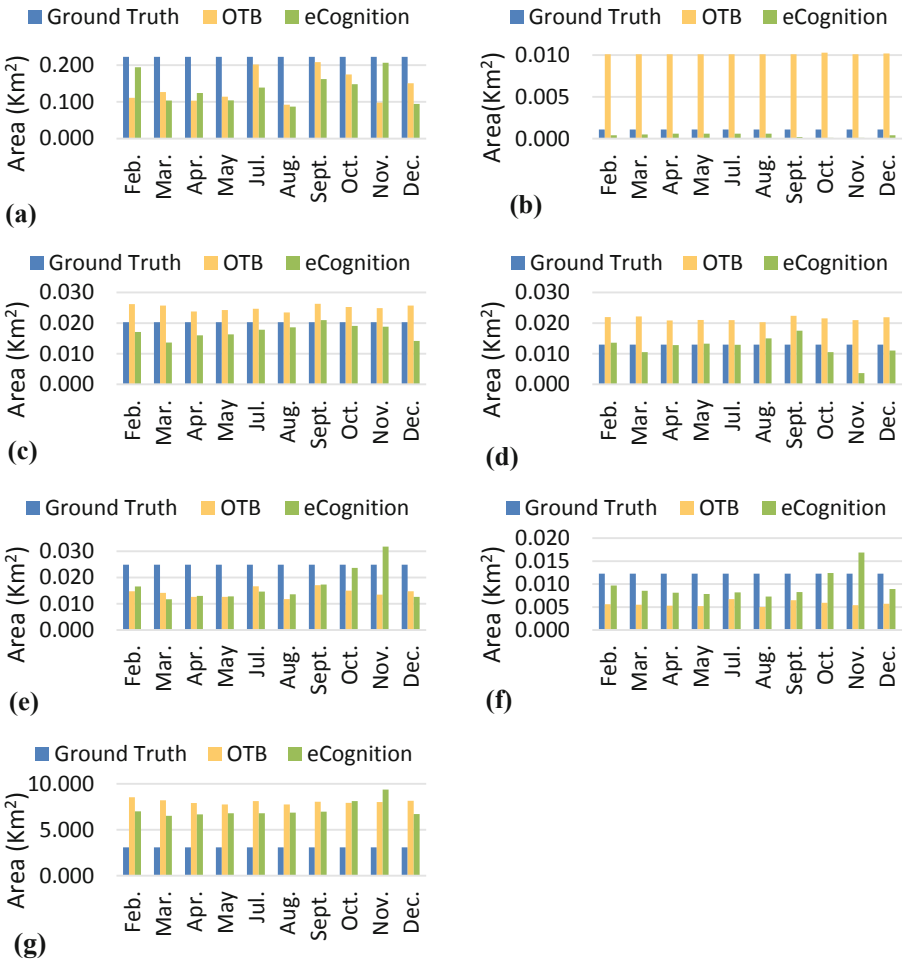


**Fig. 5.** Statistical comparison of intersecting polygon areas with GroundTruth: (a) max; (b) minimum; (c) mean; (d) median; (e) standard deviation; (f) CV; (g) Sum.

cases, the HP Pavillion Gaming Laptop 16-a0xxx computer with Intel(R) Core (TM) i7-10750H CPU @ 2.60 GHz and RAM was applied.

**Table 5.** Processing time required by eCognition Developer and OTB to segment the S2 time series.

| Software | Feb. (sec) | Mar. (sec) | Apr. (sec) | May (sec) | Jul. (sec) | Aug. (sec) | Sep. (sec) | Oct. (sec) | Nov. (sec) | Dec. (sec) |
|---|---|---|---|---|---|---|---|---|---|---|
| eCo. Dev. | 10:19.0 | 10:12.3 | 10:05.2 | 09:59.8 | 10:05.7 | 10:09.4 | 10:07.6 | 09:56.7 | 09:46.3 | 15:13.4 |
| OTB | 00:04.3 | 00:03.4 | 00:04.0 | 00:03.4 | 00:03.3 | 00:03.5 | 00:03.5 | 00:03.5 | 00:03.6 | 00:03.5 |

### 6.5 Correction Procedure Outcomes

The results in showed anomalies in October and November. For this reason, as already explained in the "Methodology" Section, the areas of the images characterized by unusual reflectance values were masked and, both segmentation algorithms were reapplied on the resultant maps. As showed in Table 6, in eCognition Developer, ED2 values were lowered compared to the original images. In OTB, on the other hand, slightly higher

**Table 6.** Correction procedure outcomes.

| | October | | | |
|---|---|---|---|---|
| | eCogntion | | OTB | |
| | Before | After | Before | After |
| **ED2** | 0.9420 | 0.4270 | 0.7150 | 0.8780 |
| **Pol.** | 2623.0000 | 4860.0000 | 2539.0000 | 2243.0000 |
| **Inters. pol. & GT ** | 425.0000 | 358.0000 | 314.0000 | 238.0000 |
| **Min ($km^2$)** | 0.0001 | 0.0004 | 0.0103 | 0.0103 |
| **Max ($km^2$)** | 0.1481 | 0.2346 | 0.1748 | 0.2346 |
| **Mean ($km^2$)** | 0.0191 | 0.0150 | 0.0253 | 0.0274 |
| **Median ($km^2$)** | 0.0105 | 0.0113 | 0.0216 | 0.0221 |
| **Dev. Sta. ($km^2$)** | 0.0237 | 0.0182 | 0.0150 | 0.0225 |
| **CV ($km^2$)** | 0.0124 | 1.2165 | 0.0059 | 0.8238 |
| **Sum ($km^{2)}$** | 8.1153 | 5.3695 | 7.9320 | 6.5130 |
| | **November** | | | |
| | eCogntion | | OTB | |
| | Before | After | Before | After |
| **ED2** | 2.8950 | 0.9420 | 1.0220 | 1.1930 |
| **Pol.** | 1979.0000 | 4703.0000 | 2586.0000 | 2250.0000 |
| **Inters. pol. & GT ** | 498.0000 | 358.0000 | 322.0000 | 240.0000 |
| **Min ($km^2$)** | 0.0001 | 0.0001 | 0.0101 | 0.0101 |
| **Max ($km^2$)** | 0.2063 | 0.2346 | 0.0982 | 0.2346 |
| **Mean ($km^2$)** | 0.0188 | 0.0164 | 0.0249 | 0.0276 |
| **Median ($km^2$)** | 0.0037 | 0.0107 | 0.0210 | 0.0211 |
| **Dev. Sta. ($km^2$)** | 0.0318 | 0.0215 | 0.0135 | 0.0228 |
| **CV ($km^2$)** | 0.0169 | 1.3100 | 0.0054 | 0.8264 |
| **Sum ($km^{2)}$** | 9.3807 | 5.8703 | 8.0228 | 6.6251 |

ED2 values were obtained in October and November than in the unmasked images. Regarding polygon statistics, in eCognition Developer, the total number of polygons is much bigger than that one reported in Table 4. This is due to scale value change (scale = 40 in October; scale = 47 in November) (see Table 2. for unmasked value). In OTB, the total polygons value did not change much. Polygons intersected with Ground Truth decreased both in eCognition Developer and OTB. Areas statistics show an increment of median value in eCognition Developer for November and a decrement of standard deviation value. This suggests that a lower number of small segments can be detected.

## 7 Discussion and Conclusion

The aim of this work was to compare the performance of the commercial software eCognition Developer with the open-source platform Orfeo ToolBox in segmenting S2 time-series covering Montalto di Castro (Viterbo, Italy). Such a zone was selected because of the presence of the largest solar park in Europe until 2011. Furthermore, to the best of the authors' knowledge, any researches have been proposed in the literature to detect PV systems from S2 images by applying OBIA. After segmented the images, the modified ED2 index was evaluated using AssesSeg software. The corresponding temporal trends of ED2 extracted using eCognition Developer and OTB were similar, except for the months of October and November where anomalies were detected and subsequently corrected. Then, polygons statistics, shown in Table 4, were computed. eCognition produced more polygons than OTB and, consequently, their intersection with Ground Truth samples was higher albeit the area sum was higher in OTB case (Table 6) This is confirmed also by the relatively high median value and relatively low standard deviation value that enhance the tendency of the mean-shift algortim to create larger polygons than Ground Truth samples. Additionally, OTB produces a narrow range of polygon sizes. Thus, polygons generated by eCognition Developer were more adapted to the selected Ground Truth samples. Although the same laptop was used to process the data, eCognition Developer showed a better performance considering that a range of parameters were tested, and non-self-intersected polygons were generated. Indeed, in the case of OTB, just single default values were evaluated and all the segmented polygons produced by OTB were characterized by self-intersected polygons, subsequently fixed. This made the process slower and complex. In addition, eCognition Developer demonstrated greater versatility and completeness in managing segmentation parameters than OTB as well as better handling heavy geospatial data. In conclusion, both software showed promising results since they generated acceptable segmentation outcomes. However, some differences have to be considered: i) eCognition Developer allowed extracting fewer large segments than those ones obtained using the other software; ii) considering the whole time needed to remove self-intersected polygons, eCognition Developer environment was faster in meeting the goal; iii) eCognition Developer amplified the anomalies detected in October and November, and, therefore, the images used in the multiresolution algorithm may be preprocessed adequately. Thus, eCognition Developer can be recognized as the optimal option for segmenting large input images. Nevertheless, its higher cost is a strong limitation in those projects characterized by a limited budget. In this case, OTB is preferable although much more time is required to produce satisfying polygons adapted for further classification purpose. In the future, other segmentation algorithms will be tested

and compared to segment Sentinel-2 images to identify the optimal strategy to adopt to improve PV parks classification accuracy.

## References


1. Heinberg, R., Fridley, D.: Our Renewable Future: Laying the Path for One Hundred Percent Clean Energy; Island Press/Center for Resource Economics: Washington, pp. 1–15. DC, USA (2016)
2. Souffer, I., Sghiouar, M., Sebari, I., Zefri, Y., Hajji, H., Aniba, G.: Automatic extraction of photovoltaic panels from UAV imagery with object-based image analysis and machine learning. In: Bennani, S., Lakhrissi, Y., Khaissidi, G., Mansouri, A., Khamlichi, Y. (eds.) WITS 2020. LNEE, vol. 745, pp. 699–709. Springer, Singapore (2022). https://doi.org/10.1007/978-981-33-6893-4_64
3. Feldman, D., Ramasamy, V., Fu, R., Ramdas, A., Desai, J., Margolis, R.: U.S. Solar Photovoltaic System and Energy Storage Cost Benchmark (2020)
4. Agrillo, A., Surace, V., Liberatore, P.: Direzione Studi e Monitoraggio di Sistema Funzione Statistiche e Monitoraggio. Gestore dei Servizi Energetici S.p.A, (2019)
5. Sahu, A., Yadav, N., Sudhakar, K.: Floating photovoltaic power plant: a review. Renew. Sustain. Energy Rev. **66**, 815–824 (2016)
6. Pindozzi, S., Faugno, S., Cervelli, E., Capolupo, A., Sannino, M., Boccia, L.: Consequence of land use changes into energy crops in Campania region. J. Agric. Eng. **44**(s2) (2013)
7. Katsikogiannis, O.A., Ziar, H., Isabella, O.: Integration of bifacial photovoltaics in agrivoltaic systems: a synergistic design approach. Appl. Energy **309**, 118475 (2022)
8. Ferrara, C., Philipp, D.: Why do PV modules fail? Energy Procedia **15**, 379–387 (2012)
9. Balzategui, J., et al.: Semi-automatic quality inspection of solar cell based on Convolutional Neural Networks. In: 2019 24th IEEE International Conference on Emerging Technologies and Factory Automation (ETFA), pp. 529–535. IEEE, September 2019
10. Zhang, D., et al.: Aerial image analysis based on improved adaptive clustering for photovoltaic module inspection. In: 2017 International Smart Cities Conference (ISC2), pp. 1–6. IEEE, September 2017
11. Wang, M., Cui, Q., Sun, Y., Wang, Q.: Photovoltaic panel extraction from very high-resolution aerial imagery using region–line primitive association analysis and template matching. ISPRS J. Photogramm. Remote. Sens. **141**, 100–111 (2018)
12. Novelli, A., Tarantino, E., Caradonna, G., Apollonio, C., Balacco, G., Piccinni, F.: Improving the ANN classification accuracy of landsat data through spectral indices and linear transformations (PCA and TCT) aimed at LU/LC monitoring of a river basin. In International Conference on Computational Science and Its Applications, pp. 420–432. Springer, Cham, , July 2016. https://doi.org/10.1007/978-3-319-42108-7_32
13. Blaschke, T.: Object based image analysis for remote sensing. ISPRS J. Photo-gramm. Remote Sens. **65**(1), 2–16 (2010)
14. Santoro, F., Tarantino, E., Figorito, B., Gualano, S., D'Onghia, A.M.: A tree counting algorithm for precision agriculture tasks. Int. J. Digital Earth **6**(1), 94–102 (2013)
15. Crocetto, N., Tarantino, E.: A class-oriented strategy for features extraction from multidate ASTER imagery. Remote Sens. **1**(4), 1171–1189 (2009)
16. Tarantino, E.: Features extraction from multi-date ASTER imagery using a hybrid classification method for land cover transformations. In: Sixth International Symposium on Digital Earth: Models, Algorithms, and Virtual Reality, vol. 7840, p. 78401T. International Society for Optics and Photonics (2010)

17. Sarzana, T., Maltese, A., Capolupo, A., Tarantino, E.: Post-processing of pixel and object-based land cover classifications of very high spatial resolution images. In: International Conference on Computational Science and Its Applications, pp. 797–812. Springer, Cham (2020). https://doi.org/10.1007/978-3-030-58811-3_57
18. Capolupo, A., Boccia, L.: Innovative method for linking anthropisation process to vulnerability. World Rev. Sci. Technol. Sustain. Dev. **17**(1), 4–22 (2021)
19. Sideris, K.: Review of image segmentation algorithms for analysing Sentinel-2 data over large geographical areas. JNCC (2020)
20. Grizonnet, M., Michel, J., Poughon, V., Inglada, J.: Mickaël, S., Cresson, R.: Orfeo ToolBox: Open source processing of remote sensing images. Open Geospatial Data, Software Stand. **2**(1), 15 (2017)
21. Xia, Z., et al.: Mapping the rapid development of photovoltaic power stations in northwestern China using remote sensing. Energy Rep. **8**, 4117–4127 (2022)
22. Khan, J., Arsalan, M.H.: Implementation of open source GIS tools to identify bright rooftops for solar photovoltaic applications–a case study of creek lanes, DHA, Karachi. J. Basic Appl. Sci. **12**, 14–22 (2016)
23. Plakman, V., Rosier, J., van Vliet, J.: Solar park detection from publicly available satellite imagery. GISci. Remote Sens. **59**(1), 461–480 (2022)
24. SMA Solar. https://www.sma-italia.com/. Accessed 21 Mar 2022
25. Infobuildenergia. https://www.infobuildenergia.it/. Accessed 15 Mar 2022
26. New tuscia. https://www.newtuscia.it/2020/06/14/. Accessed 10 Mar 2022
27. Scihub.copernicus. https://scihub.copernicus.eu. Accessed 15 Mar 2022
28. Czirjak, D.W.: Detecting photovoltaic solar panels using hyperspectral imagery and estimating solar power production. J. Appl. Remote Sens. **11**(2), 026007 (2017)
29. Trimble Geospatial Inc., https://geospatial.trimble.com/what-is-ecognition. Accessed 20 Mar 2022
30. Orfeo ToolBox. https://www.orfeo-toolbox.org/. Accessed 20 Mar 2022
31. Novelli, A., Aguilar, M.A., Aguilar, F.J., Nemmaoui, A., Tarantino, E.: AssesSeg—a command line tool to quantify image segmentation quality: a test carried out in southern spain from satellite imagery. Remote Sens. **9**(1), 40 (2017)
32. Qt. https://qt.io. Accessed 15 Mar 2022
33. QGIS Documentation. https://docs.qgis.org/3.10/it/docs/index.html. Accessed 20 Mar 2022
34. Novelli, A., Aguilar, M.A., Nemmaoui, A., Aguilar, F.J., Tarantino, E.: Performance evaluation of object-based greenhouse detection from Sentinel-2 MSI and Landsat 8 OLI data: a case study from Almería (Spain). Int. J. Appl. Earth Obs. Geoinf. **52**, 403–411 (2016)
35. Cheng, Y.: Mean shift, mode seeking, and clustering. IEEE Trans. Pattern Anal. Mach. Intell. **17**(8), 790–799 (1995)
36. Sarkar, P.R.: Comparison of Segmentation Algorithms and Estimation of Optimal Segmentation Parameters for Very High-Resolution Satellite Imagery. Indian Institute of Space Science and Technology (2016)